Supplementary Information

Field emission and anode etching during formation of length-controlled nanogaps in electrical breakdown of horizontally aligned single-walled carbon nanotubes

*Keigo Otsuka,[a] Taiki Inoue,[*a] Yuki Shimomura,[a] Shohei Chiashi[a] and Shigeo Maruyama[*a,b]*

[a] Department of Mechanical Engineering, The University of Tokyo, 7-3-1 Hongo, Bunkyo-ku, Tokyo 113-8656, Japan

E-mail: inoue@photon.t.u-tokyo.ac.jp, maruyama@photon.t.u-tokyo.ac.jp

[b] Energy NanoEngineering Lab., National Institute of Advanced Industrial Science and Technology (AIST), 1-2-1 Namiki, Tsukuba, Ibaraki. 305-8564, Japan

1. Effect of substrate heating during electrical breakdown on gap size

If the gap size formed by electrical breakdown is dominated by oxygen-induced chain reaction, substrate heating during voltage application will simply increase the gap size. Figure S1 shows the histograms of gap size at three different substrate temperatures (~20, ~60, ~100 ˚C). Contrary to the expectation, the gap size drastically decreased with increasing substrate temperature. This indicates the gap size formed by in-air electrical breakdown is not determined by chain-reaction burning. Note that slightly different maximum voltage was applied for three SWNT arrays (~60, 43, 45 V for ~20, 60, 100 ˚C, respectively). Wide distribution for lower temperature experiments may be attributed to the etching due to field enhancement between adjacent SWNTs (Figure 4) because electrical breakdown of long SWNTs (~15 μm) requires high voltage application (~60 V).

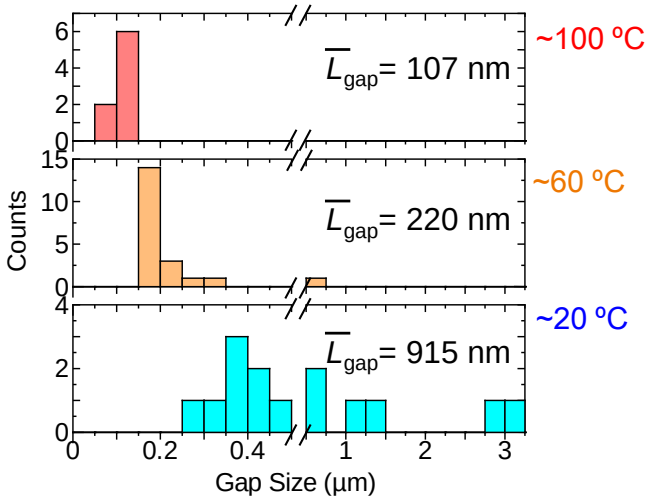

Figure S1. Distribution of gap size obtained by electrical breakdown in air at different temperatures.

2. Experimental details

We show the schematic illustration of time evolution of both voltage and gap size during gap extension experiment in Figure S2a. Voltage was increased from zero to a certain value (V_{max}: 30-100 V) typically in 100 s. Since this anode etching phenomena is self-limited due to the decreased field

enhancement associated with gap extension, the gap size seems to change with voltage. If we take a closer look at the change in voltage, it shows stepwise increase (by 30-100 mV) rather than continuous increase because of machine constraint as shown in the inset. We guess the gap size are readily increased just after each stepwise increase of voltage and keeps constant until next voltage increment. The current I and the local field at the SWNT tips F must be slightly larger than threshold (I_0, F_0) during gap growth, and then go down to threshold for a while.

To control humidity of ambient gas, pure oxygen gas or oxygen through a water bubbler was sprayed on the sample during electrical breakdown and gap extension processes. Figure S2b shows the schematic illustration of the gap extension in wet oxygen (oxygen saturated with water vapor at room temperature). Almost no water droplets were observed on the substrates by optical microscope during the wet oxygen spraying, which indicates the relative humidity of ~100%.

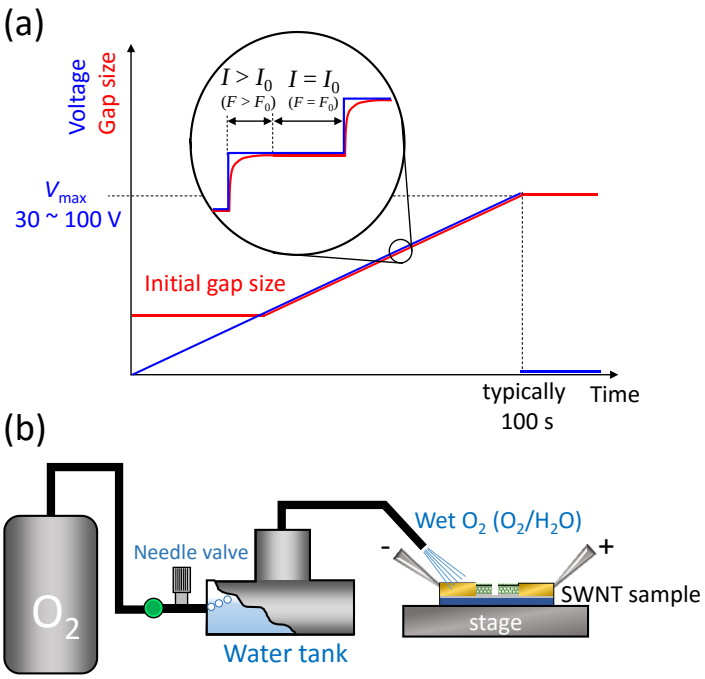

Figure S2. (a) Schematic illustration of time evolution of voltage and gap size. Inset shows the gap size change which follows the stepwise increase of voltage. (b) Schematic illustration of the gap extension in wet oxygen. Oxygen gas through a water bubbler (kept at room temperature) was directly sprayed onto the samples during the voltage application to SWNT gaps.

3. Gap extension of SWNT arrays and current transition

Throughout the study, the gaps in SWNT arrays were extended as shown in Figure S3. Red arrows indicate the gaps created by electrical breakdown process on hotplates. After further voltage application process, new gaps were formed, but not included in the calculation of the extended gap size. Some SWNTs have two gaps as second gaps are indicated by yellow arrows, probably due to the influence of adjacent gaps. Taking a closer look at the current transition during the gap extension (inset), small (~nA) and unstable current was observed after all the SWNTs were broken down ($V >$ 76 V). This current suggests the conduction through SWNT gaps which induces the gap extension.

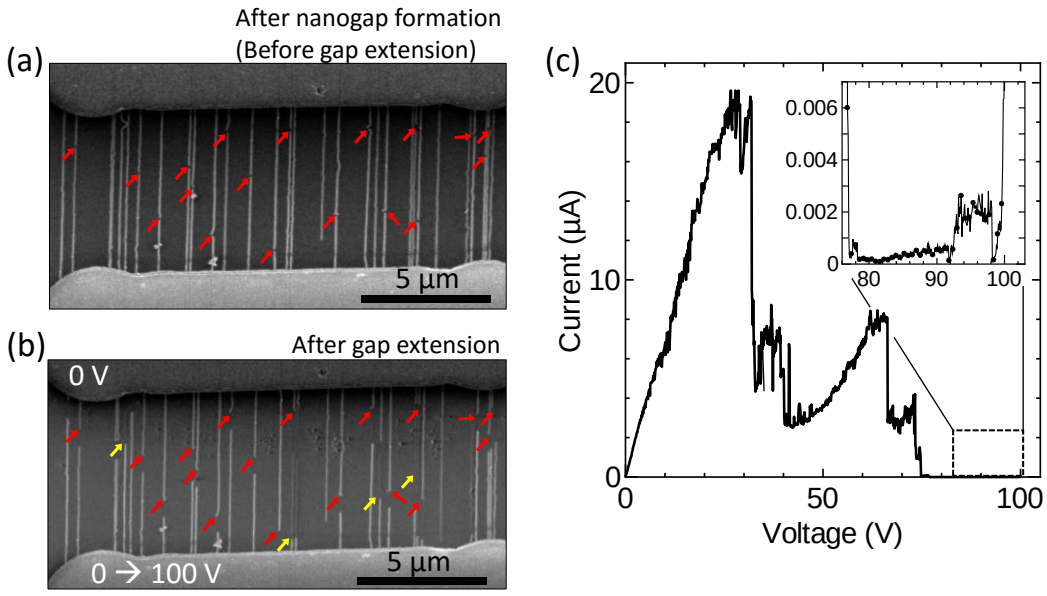

Figure S3. (a) SEM image of SWNT arrays after nanogap formation by electrical breakdown on hotplates (~100 ºC), and (b) after gap extension under ambient condition. Yellow arrows indicate the cutting of already-broken SWNTs caused by adjacent gaps. (c) Current transition during the gap extension. Inset shows enlarged graph with voltage larger than 76 V, where all the SWNTs were broken.

4. Effect of oxygen pressure during electrical breakdown on gap size

It is well known that electrical breakdown of SWNTs is affected by oxygen partial pressure.[1] With a focus on chemical reaction which induces the breakdown, higher oxygen pressure (p_{O2}) seems to lead to higher reaction rate even at the same temperature. Thus, the breakdown temperature and the breakdown power (power input needed to induce SWNT breakdown) should be high/large at low oxygen pressure.

Vacuum chamber was used to control the pressure. After evacuating the chamber (< 10 Pa) with a rotary pump, oxygen was introduced. Figure S4a shows current transition (black lines) during electrical breakdown process and the breakdown power density per unit length (blue circles). The breakdown power P_{BD} [W] was obtained by multiplying current drop ΔI [A] and applied voltage V [V] ($P_{BD} = \Delta I \times V$). The breakdown voltage and the breakdown power density were much higher at p_{O2} < 0.1 kPa than those at p_{O2} ~ 95 kPa. However, the gap size does not have clear dependence on oxygen pressure (Figure S4b). This suggest that breakdown (cutting) and gap formation of SWNTs are based on different mechanisms. Note that different V_{max} was applied for the experiments under different oxygen pressure, and the gap size was slightly dependent on V_{max} (Figure S4b inset) as described in the main article.

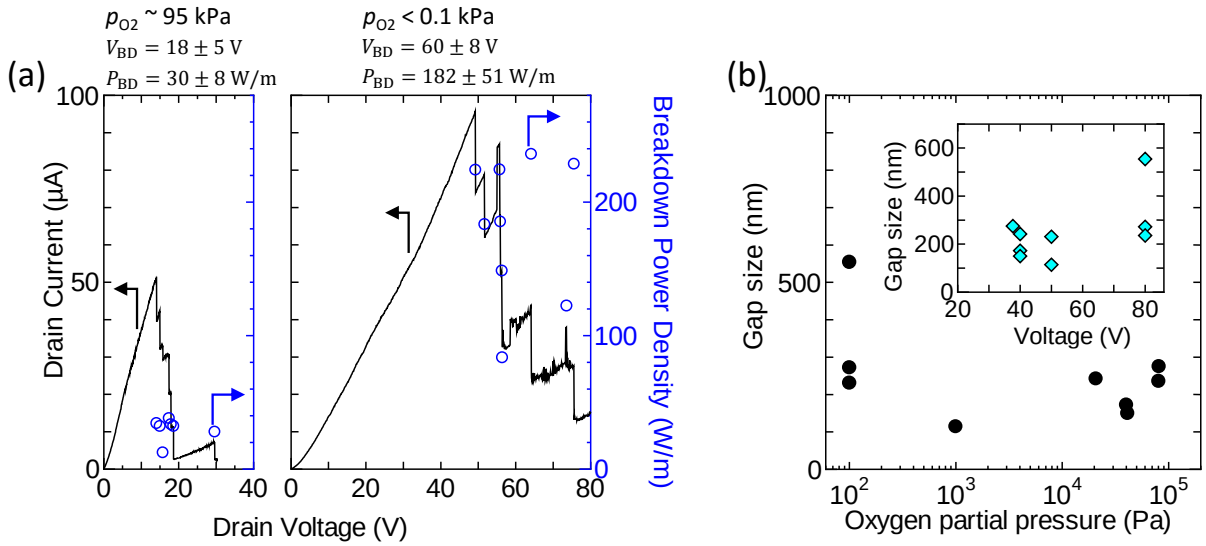

Figure S4. SWNT gaps were formed by electrical breakdown at various oxygen partial pressures (p_{O2}). (a) Current transition (black) and breakdown power density (P_{BD} [W/m], blue circle) during the electrical breakdown. (b) Oxygen pressure vs Gap size. Each data point shows the average size of typically ~10 SWNT gaps. Channel length L_{ch} = 5 μm. Inset: Gap size as a function of V_{max} shows dependence on applied voltage despite the electrical breakdown under various oxygen pressures.

5. Assumed sample configuration for field enhancement modeling

The relation between geometrical features of SWNT gaps (L_{gap} and L_{ch}) and field enhancement factor γ was obtained by fitting the experimental data shown in Figure 2. When the distance between emitter tips and anode D is large ($D > 3h$), a field enhancement factor γ_0 of the emitter shown in Figure S5a is purely a factor of the CNT height and radius and written as[2]

$$\gamma_0 \propto 1 + \sqrt{\frac{h}{2r}} \,. \qquad (1)$$

However, when D (or gap size) is small compared to SWNT length h, equation (2) will be corrected as[34]

$$\gamma = \gamma_0 \left[1 + a\left(\frac{D}{D+h}\right)^{-1} - b\left(\frac{D}{D+h}\right)\right] \quad (2)$$

Since the configuration of our sample is different from conventional field emitters, we assumed the gaps are located in the middle of channels for simplicity so that the same relation as tip-plane configuration can be used (Figure S5b). This assumption is useful also because the position of the gaps is randomly scattered around the middle of the channel.[1] Using geometrical parameters of our samples, equation (2) can be further rewritten as follows.

$$\gamma = c(1 + \sqrt{\frac{L_{\mathrm{ch}} - L_{\mathrm{gap}}}{4r}})(1 + a\frac{L_{\mathrm{ch}}}{L_{\mathrm{gap}}} - b\frac{L_{\mathrm{gap}}}{L_{\mathrm{ch}}}) \quad (3)$$

Here, three unknown parameters, *a*, *b*, and *c*, appear in the equation. The SWNTs of our samples lay on substrates as shown in Figure S5c, but we did not consider the difference between Figure S5b and c for simplicity. Since usually $L_{\mathrm{gap}} << L_{\mathrm{ch}}$ in our experiments, *b* has little effect and thus set to zero. Then proper value of a = 0.11 was obtained from V_{max} vs L_{gap} (Figure 2). Fitting lines when *a* is different (a = 0.01, 0.5) are shown in Figure S6a. Finally, *c* (= 0.66) was obtained from the field emission properties of the 80-nm-gap in vacuum and the FN law (Figure 3c). Also, *I*-*V* characteristics for the 300-nm-gap estimated from the FN law and geometrical features are shown in Figure S6b. As shown in Figure S6c, L_{ch} obtained by doubling the length of SWNT segments on cathode side $L_{\mathrm{C\text{-}SWNT}}$ (strictly speaking, $L_{\mathrm{ch}} = 2L_{\mathrm{C\text{-}SWNT}} + L_{\mathrm{gap}}$) was used to calculate field enhancement factors, which was different from the cathode-anode distance (Figure S6c). It is because we know the exact value of $L_{\mathrm{C\text{-}SWNT}}$ from SEM observation, and $L_{\mathrm{C\text{-}SWNT}}$ is more important when the field enhancement at SWNT tips on cathode side is considered. If *a* is large (for example a = 0.5), field enhancement factor γ is inversely proportional to gap size L_{gap}. At that case, gap size will be proportional to applied voltage.

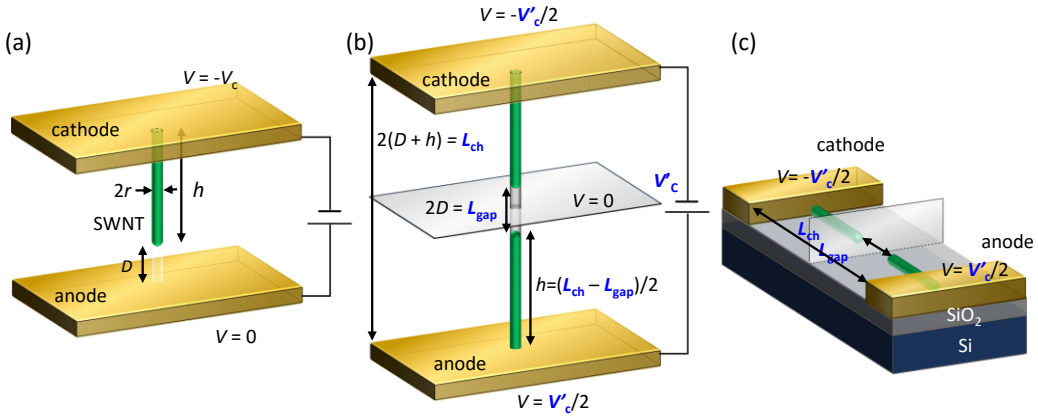

Figure S5. Schematic illustrations of sample configuration used for field enhancement modeling. (a) Typical configuration with SWNT tip-to-flat metal electrode. (b) Tip-to-tip configuration (free standing) assuming the gap is located at the center. (c) SWNT gap on substrates (our samples).

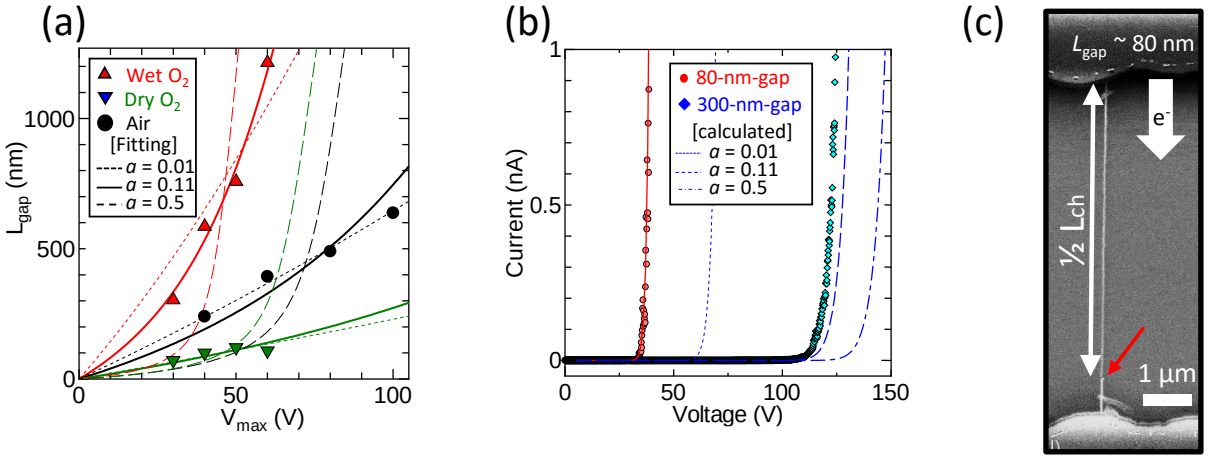

Figure S6. (a) Fitting lines of the data shown in Figure 2 with the equation [$V_{max}(L_{gap}) = F_0 L_{ch}/2\gamma$], which give the constant local field F_0 for variable gap size. a and F_0/c are fitting parameters. (b) Predicted field emission current for the 300-nm-gap. Dotted lines, dashed lines, and dash-dotted lines are obtained when a = 0.01, 0.11, 0.5 in equation (2), respectively. (c) SEM image of the 80-nm-gap. The gap was not located in the middle.

6. Extrapolation of threshold current for gap extension

The current needed for the gap extension is too small to detect. When ramp voltage was applied to a single gap in air, usually no current was detected. We estimated the minimum current (threshold

current) needed to extend the SWNT gaps in air by extrapolating the FN plots obtained in vacuum. Field emission current can be simply expressed by two constants and voltage as $I = C_1V^2\exp(-C_2/V)$. Figure S7a and b show the fitting in an *I*-*V* curve and an FN plot, respectively. The fitting and extrapolation of the gap in Figure 3e (red) yields threshold current (at V = 20 V) of 0.56-1.70 fA. Also, the gap in Figure 3e (blue) gives similar threshold current of 0.33 fA (Figure S7c). We should note that this estimation is appropriate unless C_1 and C_2 are affected by water, oxygen, nitrogen, and so on.

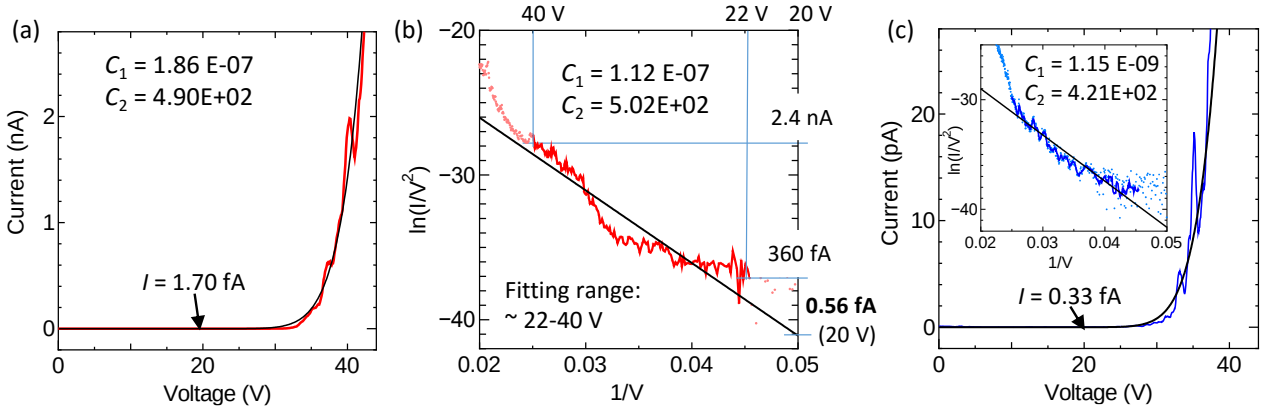

Figure S7. (a) Fitting line for the experimental *I*-*V* characteristic [in red in Figure 3(c)] with the FN law [$I = C_1V^2\exp(-C_2/V)$]. (b) Similar fitting for the FN plots for the same gap. Since the gap was extended by bias voltage of V = 20 V, these fittings yield the threshold current for gap extension in air of I = 0.56 – 1.70 fA. (c) The same fitting was applied to the gap drawn in blue in Figure 3(e). This gap yields the threshold current of I = 0.33 fA.

7. Strategy for full length and selective etching of m-SWNTs utilizing field emission

Site-controlled formation of gaps of m-SWNTs and s-SWNTs could be used for selective elimination of m-SWNTs in full length. A possible process is shown in Figure S8. Breakdown position of m-SWNTs can be easily controlled by depositing intermediate electrodes (drawn in gray in Figure S8b). The intermediate electrodes are selectively etched after the gap formation in m-SWNTs. Then,

site-selective cutting of s-SWNTs can be done, for example, by passivating large area of channel region to protect SWNTs from oxygen, except for near anodes (Figure S8c). After removing passivation layers, high voltage is applied in wet gas ambient (Figure S8d). All m-SWNTs can be removed in full length, as long as inter-SWNT spacing is small enough (Figure S8e). On the other hand, some m-SWNTs on anode side cannot be etched if the SWNT density is too small (Figures S8f and g).

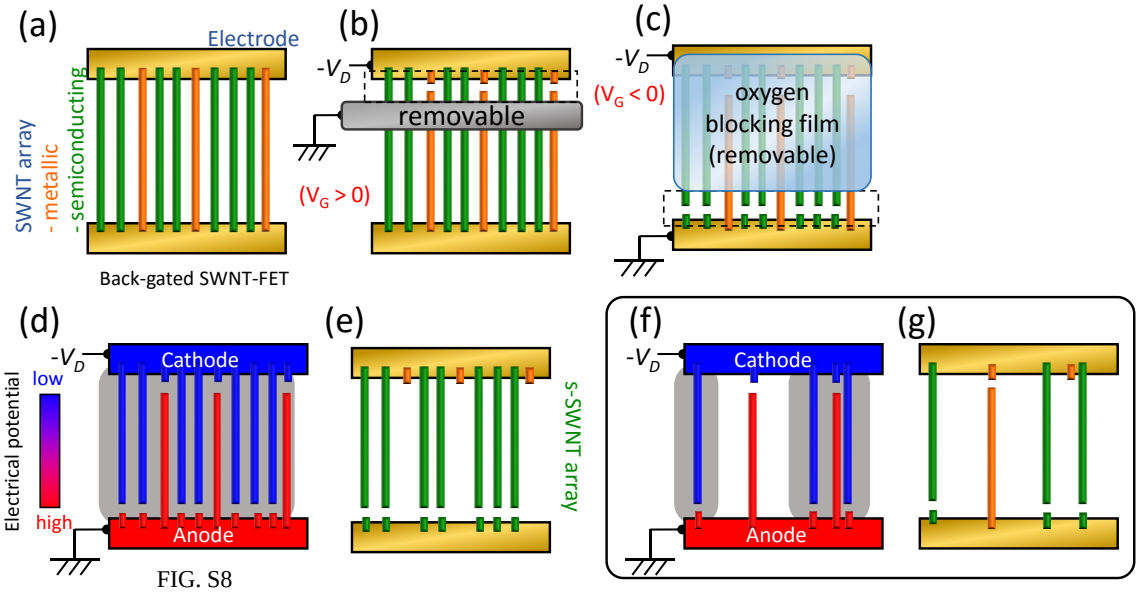

Figure S8. Schematic illustration of the potential application of A-SWNT etching by side walls of adjacent C-SWNTs. (a) Initial SWNT arrays. (b) Electrical breakdown of m-SWNTs near cathodes, and (c) following breakdown of s-SWNTs near anodes while voltage-driven etching is suppressed. (d) High voltage application to etch A-SWNTs (supposedly m-SWNTs) under wet gas condition. (e) s-SWNT arrays. (f,g) If the density of SWNT arrays is small, some A-SWNTs cannot be removed.

References

1 A. D. Liao, R. Alizadegan, Z.-Y. Ong, S. Dutta, F. Xiong, K. J. Hsia and E. Pop, *Phys. Rev. B*, 2010, **82**, 205406.

2 R. C. Smith, D. C. Cox and S. R. P. Silva, *Appl. Phys. Lett.*, 2005, **87**, 103112.

3 C. J. Edgcombe and U. Valdrè, *J. Microsc.*, 2001, **203**, 188–194.

4 J.-M. Bonard, K. Dean, B. Coll and C. Klinke, *Phys. Rev. Lett.*, 2002, **89**, 197602.